Journal of Thermal Analysis and Calorimetry, Vol. 60 (2000) 957–974

PROSPECTS OF MATERIALS SCIENCE
From crystalline to amorphous solids

H. Suga

Research Institute for Science and Technology, Kinki University, Kowakae, Higashi-Osaka
577-8502, Japan

Abstract

A survey of materials science through our experiences shows that our knowledge of amorphous solids is quite poor compared with that of crystalline solids. Most pure substances can be obtained, in principle, as crystalline as well as non-crystalline states by physical and chemical methods. Destruction of the three-dimensional periodicity in crystalline substances will produce novel properties which cannot be anticipated from knowledge of crystal sciences. One direction of materials science in the coming century will surely be a new realm of amorphous condensed matter science.

Keywords: crystals, glass transition, non-crystalline solids, residual entropy

Introduction

It was 1912 when Laue discovered that an X-ray beam was scattered by crystalline substances in a regular way depending on the spatial arrangements of atoms in the crystals. Aided by advanced computer techniques, X-ray crystallography has developed to a highly sophisticated level. Many physico-chemical properties of substances are now understood based on structural information. Neutron diffraction added valuable information, particularly to the positions of protons involved in hydrogen-bonded crystals. These structural data have been well-documented in databases which are easily accessible by personal computer. In this sense, the solid-state sciences that have developed greatly in the 20th century have actually meant crystal sciences.

Glasses, as one category of amorphous solids, were discovered in the ancient Egyptian era. In spite of their important technical applications, the glass transition temperature, T_g, that was one characteristic feature of glasses, was not observed until 1933. It is surprising to realize that the experimental observation of T_g is a more recent event than the discovery of radioactivity. Unfortunately, the X-ray diffraction method was not powerful enough for any solids that lack three-dimensional periodical arrangements of the constituents. Glasses have been one of the exceptional cases of validity of the third law of thermodynamics, owing to some frozen-in degrees of freedom.

1418–2874/2000/ $ 5.00

Akadémiai Kiadó, Budapest
Kluwer Academic Publishers, Dordrecht

In this article, I will follow first the development in crystal sciences through our experiences and then stress the importance of clarification of the unique features displayed by amorphous solids.

Transition phenomena in solids

Phase transitions in crystals

One of the fascinating phenomena observed in crystals is a phase transition by which many of the physical properties such as electric, magnetic, mechanical, optical and others change slightly or drastically. A phase transition of a crystal was first observed for sulphur in the 18th century. the phenomenon might be regarded as unusual at that times. Since then various kinds of phase transitions have been the subject of theoretical and experimental physics and chemistry of crystalline materials. It would be difficult, nowadays, to find a crystal that does not exhibit any polymorphism over a wide range of temperature and pressure. Research activity on phase transitions was undoubtedly accelerated by structural studies below and above the transition temperature T_{trs}. The high-temperature phase above T_{trs} is characterized by an entropy increase, due to the onset of orientational, conformational, and/or positional disordering of the constituent atoms, ions, or molecules.

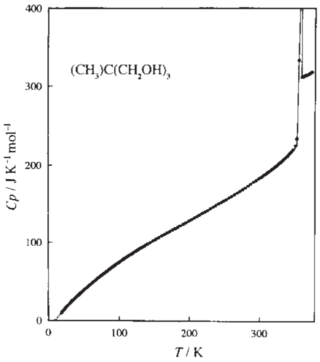

Fig. 1 Heat capacity of neopentanetriol

The nature of the disorder and the dynamic situation of the constituents are clarified by entropy considerations as well as dielectric, NMR, Raman, and IR spectroscopies [1]. From a thermodynamic point of view, the equilibria between any two phases of a substance, separated by discontinuities in volume *V*, enthalpy *H*, and so on, are described well by the Clausius–Clapeyron equation. A phase transition with continuity in *V*, *H* etc., but with discontinuities in thermal expansivity α, heat capacity, C_p, and isothermal compressibility κ_T, was treated theoretically by Ehrenfest and designated as a second-order phase transition. A typical example of a second-order transition was provided by superconducting transitions in some metals observed at the beginning of the 20th century. The heat capacity of the superconducting phase drops suddenly at a critical temperature, T_c, which separates the normal-conducting phase at higher temperatures. Phase transitions provide typical examples of the cooperative phenomena generally occurring in condensed matters.

Figure 1 plots the molar heat capacity of a neopentanetriol $(CH_3)C(CH_2OH)_3$ crystal *vs.* temperature. A first-order transition occurs at 358.2 K [2]. The high-temperature phase belongs to an fcc system and the enthalpy of transition $\Delta_{trs}H$=21.2 kJ mol^{-1} is much larger than that of fusion $\Delta_{fus}H$=4.7 kJ mol^{-1}. The molecule in the lattice has a point group of C_{3v} at the most through the internal rotation. In order to fulfill the O_h site symmetry, a C_{3v} molecule must take up at least eight equi-energetical orientations by aligning all the C–C bonds in the molecule to the body-diagonal directions at each site of the cubic lattice. The contribution from the orientational degree of freedom to the entropy of transition, $\Delta_{trs}S$, can be expressed as Rln8 in the Boltzmann expression, where R is the gas constant. The amount is too small to account for the entropy of transition.

All the homologous compounds, $(CH_3)_{4-n}C(CH_2OH)_n$, undergo the corresponding phase transition. The transition temperature, T_{trs}, increases systematically with n, the number of hydroxymethyl group in each molecule, from 140.0 K for $C(CH_3)_4$ to 461.6 K for $C(CH_2OH)_4$. The entropy of transition, $\Delta_{trs}S$, also increases with n from 2.21R for $C(CH_3)_4$ to 10.8R for $C(CH_2OH)_4$. In contrast, the entropy of fusion $\Delta_{fus}S$ is almost constant irrespective of n. The average value (1.3±0.2)R is less than those of monoatomic crystals such as Ar (1.64R), Kr (1.70R), and Xe (1.71R). All the compounds are waxy and soft in their high-temperature phases and belong to the category of plastic crystals defined originally by Timmermans [3]. Interestingly, nearly all the transitions are accompanied by a heat capacity jump $\Delta_{trs}C_p$, which exhibits a maximum value at n=3. This behaviour attracts our academic interest for explaining microscopically the thermodynamic quantities in terms of the onset of orientational and conformational disordering of molecules at the transition. This is because each molecule possessing $-CH_2OH$ group can produce new conformers by rotating around the C–C and C–O axes. From a practical point of view, some of these materials may be used as a heat reservoir which absorbs or releases latent heat while maintaining the respective transition temperature. Since plastic crystals are mutually miscible, modification of their ability as heat reservoirs will be possible by mixing some of them. These crystals can be combined with solar energy systems to form passive solar heating materials [4].

Figure 2 shows the molar heat capacity of potassium ferrocyanide trihydrate $K_4Fe(CN)_6\cdot 3H_2O$, which exhibits a ferroelectric-paraelectric transition at 248.6 K. The crystal has a layer structure which consists of hydrogen-bonded water layers sandwiched between two double layers composed of ferrocyanide octahedral and potassium ions. Since the anhydrous compound does not show any anomalous heat capacity between 13 and 300 K, water molecules play an important role through the formation of hydrogen bonds in the manifestation of the ferroelectricity, as in the case of KH_2PO_4 and other crystals. Its deuterate analogue $K_4Fe(CN)_6\cdot 3D_2O$ undergoes the same transition at 255.1 K, showing a slight positive isotope effect on T_{trs}. The entropy of transition is of the order of $R\ln4$, and can be interpreted by the water trimer possessing four different configurations with respect to the hydrogen atoms involved in the O···O and O···N hydrogen bonds [5].

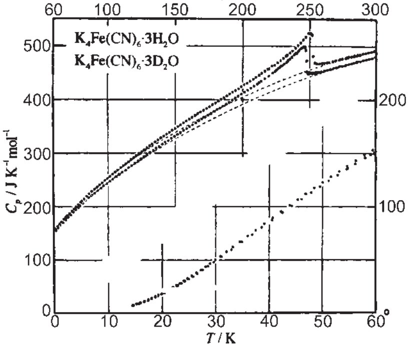

Fig. 2 Heat capacities of $K_4Fe(CN)_6·3H_2O$ and $K_4Fe(CN)_6·3D_2O$

The heat capacity drops suddenly at the transition without showing any divergence. This suggests that the transition should be second-order. To examine the possibility, the following Ehrenfest equation was tested by measuring the volume V around the T_{trs}.

$$\left(\frac{\mathrm{d}p}{\mathrm{d}T}\right)_{trs}=\frac{\Delta C_p}{T_{trs}V\Delta\alpha}, \tag{1}$$

where ΔC_p and $\Delta\alpha$ are the jumps in the heat capacity and thermal expansivity at the T_{trs}, respectively. Substitution of experimental data into the equation gives $3.22·10^7$ N m^{-2} K^{-1} for $(\mathrm{d}p/\mathrm{d}T)_{trs}$. This value is to be compared with $3.77·10^7$ N m^{-2} K^{-1}, the direct data of $(\mathrm{d}p/\mathrm{d}T)_{trs}$, observed by Krasnikova *et al.* [6]. In view of the fact that the quantities in the right-hand side of the equation were obtained by taking derivatives of H and V with respect to T, we can regard the present phase transition as being second-order or very close to it. An aniline hydrobromide, $C_6H_5NH_3Br$, crystal undergoes a ferroelectric to paraelectric phase transition at 300 K with a discontinuous drop in the heat capacity. Again the transition is believed to be almost second-order [7].

Critical phenomena can be observed not only at the critical points of liquid–vapour equilibria, but also in many solid-solid transition points. The first example was given by the antiferromagnetic-paramagnetic transition in $CoCl_2·6H_2O$ occurring at T_N=2.289 K [8]. The phenomena became one of the most important subjects in statistical mechanics [9]. Here we can give an example of an antiferroelectric-paraelectric transition observed in stannous chloride dihydrate $SnCl_2·2H_2O$ crystal at 218 K. The crystal has a layer structure composed of alternating $SnCl_2$ and water layers [10]. The water layer has four-membered and eight-membered hydrogen bonded rings giving rise to a two-dimensional, 4–8 hydrogen-bonded network. Each proton has two stable sites along each hydrogen bond and occupies the sites following the ice rules proposed by Bernal and Fowler [11]. The transition is essentially due to an order-disorder process of the protons in the two-dimensional network.

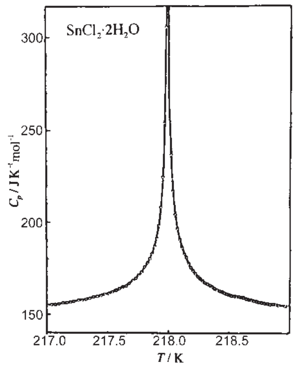

Fig. 3 Heat capacity divergence observed around T_c of $SnCl_2·2H_2O$

Figure 3 gives the molar heat capacity of a single-crystalline sample of $SnCl_2·2H_2O$, experimentally determined with a temperature resolution of 5 μK. The heat capacity exhibits a strong divergence towards T_c from both sides of the transition temperature, with highly symmetrical shape. The symmetrical divergence is a trademark of two-dimensionally interacting systems. The heat capacity divergence can be analyzed in terms of the following equation that has a theoretical justification [12].

$$\Delta C_p(T)=\frac{A}{\alpha}\left(\left|\frac{T-T_c}{T_c}\right|^{-\alpha}-1\right) \tag{2}$$

The parameters, T_c the critical temperature, α the critical exponent and A the critical amplitude, can be determined by a curve-fitting procedure. The following values were obtained (prime means the value above T_c): $\alpha=\alpha'=0.492$, $A=0.565$ J K^{-1} mol^{-1}, and $A'=0.568$ J K^{-1} mol^{-1}. The relations $\alpha'/\alpha=1.000$ and $A'/A=1.005$ validate the picture of a two-dimensional interaction.

Salinas and Nagle [13] have treated this proton order-disorder process as a planar dimmer model and solved it exactly. The exact solution, however, required a particular ground-state proton configuration for there to be a phase transition. The proposed configuration turned out to be exactly the same as the one determined by a later neutron diffraction experiment. The theory gave a highly symmetric heat capacity anomaly with a logarithmic divergence ($\alpha=\alpha'=0$) which is weaker than that observed experimentally. An unusual property of the transition is that no change in symmetry of the crystal structure occurs below and above T_c. The proton disordering proceeds with raised temperature while keeping the same crystal symmetry. It is generally observed that one or more of the symmetry elements disappear as the substance under-

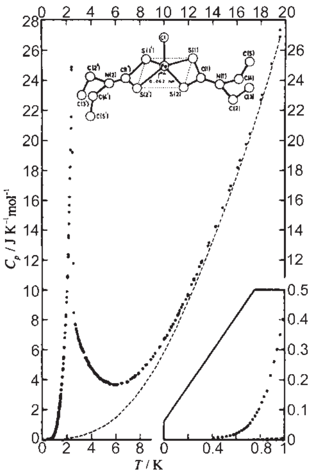

Fig. 4 Heat capacity of bis(N,N-diethyldithiocarbamate)-iron(III) chloride

goes any phase transitions. In this sense, the crystal $SnCl_2 \cdot 2H_2O$ provides an intriguing example of an isomorphous phase transition.

Figure 4 shows the heat capacity of polycrystalline bis(*N,N*-diethyldithiocarbamate)-iron(III) chloride $Fe(C_{10}H_{20}N_2S_4)Cl$ [15] which undergoes a ferromagnetic-paramagnetic transition at T_c=2.412 K. Interestingly, the corresponding bromide and iodide exhibit antiferromagnetism below T_N=0.34 and 1.90 K, respectively. The coordination geometry around the central iron(III) and the magnetic exchange interaction among the complexes seriously affect their magnetic properties. These transitions occur at very low temperatures so that the magnetic heat capacity can be separated easily from the lattice-vibrational one. This situation is one of the merits of studying phase transitions arising from weak intermolecular interactions. The heat capacity diverges towards T_c from both sides of temperature, but analysis of the critical exponent was not possible for a polycrystalline sample, owing to various kinds of involved physical defects which damage the true critical character in the vicinity of T_c.

However, the entropy change associated with the transition is not sensitive to these kinds of lattice defects. Magnetic spin is a well-quantized quantity and the corresponding entropy of transition clarifies the spin quantum number, s . The entropy of transition 11.20 J K^{-1} mol^{-1} is quite close to $R\ln 4$. Thus the magnetic ground state turns out to be a quartet with s=3/2. Octahedral iron(III) complexes possessing a $(3d)^5$ electronic configuration can generally exhibit either one unpaired electron with a doublet ground state of s=1/2, or five unpaired electrons with a sextet ground state of s=5/2, depending on the ligand field. In this sense, the present chloride is characterized by an intermediate spin manifold of 4.

The glass transition in amorphous solids

Most of the solid materials surrounding us are in a non-crystalline or amorphous state. Amorphous solids combine a liquid-like disordered structure and a crystal-like rigidity, and display unique features that are generally absent in their counterparts in crystalline materials. The glass transition, residual entropy, structural relaxation, and crystallization are important keywords for the characterization of amorphous solids [16]. Historically, the glass transition has been observed in undercooled liquids and, therefore, is regarded as a characteristic property of liquids. Later experiments, however, showed that the phenomenon is quite common in amorphous solids prepared by various methods other than the traditional liquid-cooling [17].

These non-traditional methods are divided conveniently into physical and chemical methods. Physical methods include condensation of vapour onto a cold substrate, mechanical grinding of crystal, and bombardment of a crystal with high-energy particles. Chemical methods include rapid precipitation by chemical reaction, dehydration of a hydrate crystal, desiccation of gels and so on. In the latter methods, the chemical potential of the system is modified by the change in chemical composition, while the composition is unchanged in the physical methods. Solid-state amorphization of crystals is particularly useful for materials which undergo decomposition on heating before reaching a hypothetical fusion temperature [18]. These materials have many important applications in advanced technology, such as optical fibers in telecommunication, amorphous semiconductors in solar cells, freeze-drying of pharmaceuticals and biologicals. The stability of drugs is greatly improved by embedding them in a vitreous matrix. The basic understanding of the state of aggregation of the constituent entities in these solids is quite poor compared with that in crystalline solids. There are two main reasons. The first is due to the difficulty in dealing with a frozen-in disordered system arising from the non-unique nature of any physical quantities, even under the specification external variables, as is described later. An innumerable number of structures exist in a liquid. Thus states depend strongly on the manner by which the state was realized. This situation differs much from that of the crystalline state. Erroneous conclusions will be reached when two experimental results on the same, but differently-prepared, samples are compared without particular caution.

The second reason arises from the difficulty in determining their structures by traditional methods, such as X-ray and neutron diffraction techniques. Important structural information contained in the many Bragg peaks for crystalline solids is buried mostly in a halo pattern for non-crystalline solids. Still, the radial distribution function, obtained from the halo pattern with the help of theoretical methods, gives some important information on the short-range order, or the size of ordered clusters, which are considered to control the rate of structural relaxation in non-crystalline solids. However, the derived radial distribution function is not sensitive to changes in short-range order. It is almost impractical at the present moment to compare various relaxation data with the changes in short-range order developed in vitreous solids. Other experimental techniques such as EXAFS are under progress for studies of the structures of liquid and glasses, and are expected to play an important role in the clarification of the nature of the short-range order characteristic of any disordered condensed matters in future. The poor structural information of disordered solids will be supplemented essentially by rapidly-growing computer simulation techniques. A recent paper by Uchino *et al*. [19] might be interesting in the determination of the shape of small ordered clusters which are the origin of sharp peaks observed in the Raman spectra for fused silica.

Under such circumstances, we have to rely on low-temperature calorimetry for the characterization of vitreous solids, because adiabatic calorimeters can detect all the key phenomena described above, and work particularly well as a low-frequency spectrometer for the structural relaxation [20]. Low-temperature calorimetry does not measure the heat capacity of a substance, but actually measures the enthalpy function H of the substance as a function of temperature T. The heat capacity C_p is calculated simply from the derivative of H with respect to T at constant pressure.

A constant calorimetric temperature under adiabatic conditions is a prerequisite for thermal equilibrium. This is always confirmed during the equilibrium period in adiabatic calorimetry with a discontinuous heating mode. If the calorimetric temperature happens to change spontaneously with time during the equilibration period, it reflects occurrence of an irreversible process in the sample, relaxing from a non-equilibrium to an equilibrium state. An excess amount of enthalpy, produced by a frozen-in degree of freedom of the sample, will be released towards the equilibrium value and causes a spontaneous change in the sample temperature under adiabatic conditions. The enthalpy of any disordered system can be divided into two parts: configurational enthalpy H_{conf} and vibrational enthalpy H_{vib}. The latter responds quickly to the variation of temperature in the whole range of temperature, while the response time of the former increases rapidly with decreasing temperature. It is this part of the enthalpy which causes freezing of the system below a certain temperature interval called the glass transition temperature T_g. The enthalpy of the substance can be kept constant under adiabatic conditions. Thus we have the following equations.

$$\begin{aligned} &H_{\mathrm{conf}}+H_{\mathrm{vib}}=\text{constant} \\ &\frac{\mathrm{d}(\Delta H_{\mathrm{conf}})}{\mathrm{d}t}=-\left[\frac{\mathrm{d}(\Delta H_{\mathrm{vib}})}{\mathrm{d}T}\right]\frac{\mathrm{d}T}{\mathrm{d}t}=-C_{\mathrm{vib}}\frac{\mathrm{d}T}{\mathrm{d}t} \end{aligned} \tag{3}$$

where the vibrational heat capacity C_{vib} can be obtained as that measured below T_g. The frozen-in configurational enthalpy will relax at a rate described by the following Kohlrausch-Williams-Watts' empirical equation [21].

$$\Delta H_{\mathrm{conf}}(t)=\Delta H_{\mathrm{conf}}(0)\exp\left(\frac{t}{\tau}\right)^{\beta} \tag{4}$$

where τ is the structural relaxation time and β is designated as the non-exponentially parameter. Combination of both equations leads to the following equation

$$T_{\mathrm{vib}}(t)=a+bt+c\exp\left(-\frac{t}{\tau}\right)^{\beta} \tag{5}$$

In this way, analyses of the spontaneous temperature changes observed in any equilibration periods give the data of τ and β as a function of temperature.

Some aliphatic hydrocarbon liquids are known to be good glass-formers. This is particularly true for 1-olefins because head-to-tail reorientational motion of the molecules required for the nucleation and growth of crystals becomes very slow as the temperature is lowered. Propene has the lowest T_g value of 55 K. The molar heat capacities of 1-pentene (CH_2=$CHCH_2CH_2CH_3$), prepared *in situ* by two different methods, vapour-deposition (VQ) and liquid-quenching (LQ), are drawn in Fig. 5 [22]. In both cases, the heat capacity below T_g was determined by extrapolating the spontaneous temperature drifts to the midpoint of each energizing period. Therefore the heat capacity data correspond to the 'instantaneous' or 'iso-configurational' ones which are equal to the vibrational heat capacity. The data above T_g, where the structural relaxation are short enough, were obtained until thermal equilibrium was realized during each equilibration period. Thus the data involve a contribution from the configurational enthalpy. For this reason, both the heat capacity data below and above T_g coincide well.

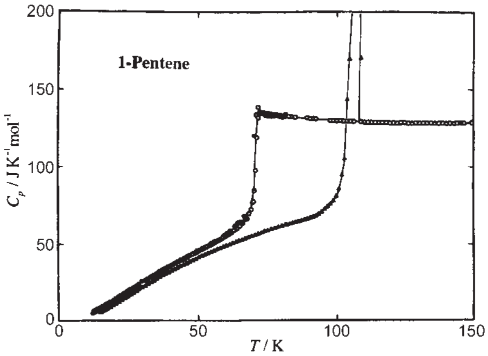

Fig. 5 Heat capacities of 1-pentene. • – VQ solid: ○ – LQ solid: Δ – crystal

However, the excess configurational enthalpy stored in both solids differs much in its magnitude. The relaxation enthalpy observed during the equilibration period can be calculated from the period of observation multiplied by the rate of temperature change. The quantity is summed over the relevant temperature range to give the total amount of relaxed configurational enthalpy H_{conf}, or simply H_c. The results are given in Fig. 6 as a function of temperature. The configurational enthalpy of VQ solid, 1 kJ mol^{-1}, is much greater than that of LQ solid, 0.15 kJ mol^{-1}. The relaxation enthalpy of VQ solid starts at deposition temperatures of 50 K (far below T_g), while that of LQ solid appears at temperature 10 K below T_g. We have already observed that for butyronitrile [23] the amount of excess configurational enthalpy depends on the deposition temperature. The lower the temperature of deposition, the larger the configurational enthalpy. In this way innumera-

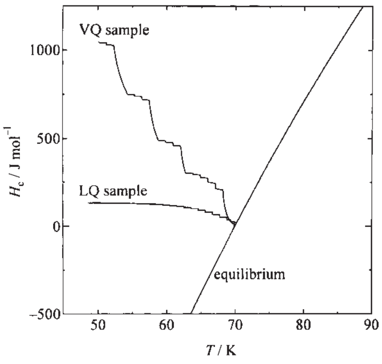

Fig. 6 Configurational enthalpy H_c of VQ and LQ 1-pentene solids plotted *vs*. temperature

ble non-crystalline solids with continuous hierarchical energies, will be possible to prepare by changing the experimental conditions.

This classical picture is incompatible with the recent discovery of high-density and low-density amorphous ices, prepared by changing the pressure at low-temperatures [24]. The two 'modifications' of amorphous ice can transform into each other in a reversible way. Ice I_h is composed of full hydrogen-bonds formed in a tetrahedral arrangement of oxygen atoms with the wurzite-type structure. For this reason, ice I_h has an unusually open structure. This modification is possibly formed at the cost of van der Waals interaction energy. Most probably the formation of high-density amorphous ice is possible at the cost of hydrogen-bonded energy. The normal critical point of H_2O separates the high-density amorphous H_2O called water, and the low-density amorphous H_2O, called steam. It is not unimaginable to assume a second critical-point on one branch of the equilibrium line which separates two water liquids [25, 26]. This situation reminds us of the models of dense-random-packing and loose-random-packing of spheres proposed by Bernal. Research on 'polyamorphism' is a challenging novel problem in the physics and chemistry of non-crystalline solids.

The structural relaxation rate can be analyzed in terms of the entropy theory [27] proposed by Adam and Gibbs for undercooled liquids. They gave an expression for the configurational relaxation time τ as a function of the configurational entropy S_c, and the temperature, T, in the following form.

$$\tau=\tau_o \exp\left(\frac{\Delta\mu s_c^*}{k_B T S_c}\right) \tag{6}$$

or its logarithmic form

$$\ln\frac{\tau}{\tau_o}=\frac{\Delta\mu s_c^*}{k_B T S_c} \tag{7}$$

where k_B is the Boltzmann constant, $\Delta\mu$ the activation Gibbs energy per mole, and s_c^* the configurational entropy of the subsystem (cluster) capable of changing its configuration cooperatively. The slowing down of the exothermic enthalpy-relaxation rate observed calorimetrically can be a result of decreasing S_c during each annealing process.

The exothermic enthalpy relaxation of the VQ solid can be analyzed by this equation. The relaxation time at each instant is assumed to be identical with the effective relaxation time defined by Kovacs [28] as follows.

$$\tau_{\mathrm{eff}}(t)=\frac{-\frac{\mathrm{d}H_c}{\mathrm{d}t}}{\Delta H_c(t)} \tag{8}$$

Plots of $\log\tau_{\mathrm{eff}}$ *vs.* $(TS_c)^{-1}$ are displayed in Fig. 7 for several temperatures at which the relaxation rates were followed over a long period. Since the numerator of the right-hand side of Eq. (7) is considered to be practically constant in each process, the plots are expected to be linear. This is exactly what happened in the actual analysis. The plot also gave a straight line for the LQ solid. This gives evidence for the wide applicability of the entropy theory.

Residual entropy S_0 is another important quantity for the characterization of non-crystalline solids. The value quantifies the extent of frozen-in disorder in the vitreous solid. The residual entropy can be obtained by a loop calculation of the integration along the thermodynamic path: crystal (0 K) – liquid – undercooled liquid – glass (0 K). The results for 1-pentene are drawn in Fig. 8. Here a small correction, arising from the difference in vibrational entropies between the crystalline and non-crystalline solids, is taken into account. Another correction for entropy production arising from the irreversible structural relaxation during the heat capacity measurement is necessary. For an LQ solid such as isopentane, the amount turned out to be negligibly small compared with the experimental uncertainty [29]. Thus the correction was ignored in the present LQ solid. For the VQ solid, the residual entropy was determined by using the concept of fictive temperature proposed by Tool [30]. The actual value of S_0 is 19.7 J K^{-1} mol^{-1} for the LQ solid, and 31.7 J K^{-1} mol^{-1} for the VQ solid.

A survey of the literature shows few examples (less than 20) of non-crystalline solids for which the residual entropy has been determined. It is highly desirable to collect much S_0 data for non-crystalline solids prepared by LQ, as well as other

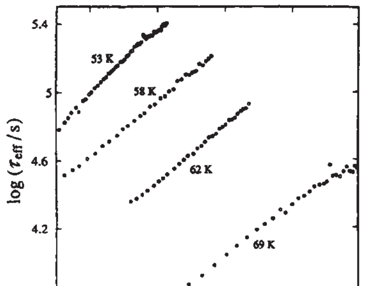

Fig. 7 Structural relaxation time of 1-pentene VQ solid plotted *vs.* $(TS_c)^{-1}$

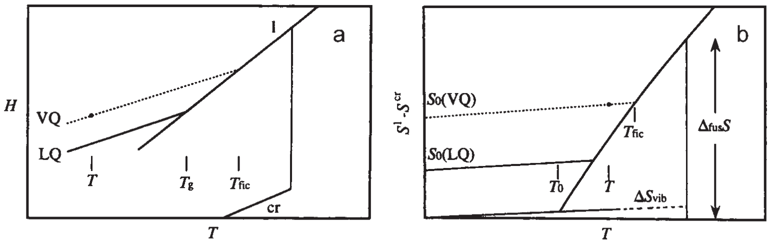

Fig. 8 Fictive temperature T_{fic} (a) and residual entropy (b) of 1-pentene

non-traditional methods, in order to quantify the different nature of frozen-in disorder of the constituent entities in respective non-crystalline solids.

The value of S_0 is related to the entropy of fusion $\Delta_{fus}S$ and the heat capacity jump ΔC_p at T_g. The discontinuous change in heat capacity differs much from substance to substance. The jump in C_p will reflect the 'relaxing entity' frozen at T_g, but it is not easy to normalize the heat capacity such that the discontinuity of the normalized heat capacity becomes constant among many liquids. Angell has considered the relation between the value of ΔC_p at T_g and the behaviour of the viscosity η of glass-forming liquids. In general, the greater the ΔC_p, the larger the slope of $\ln\eta$ plotted *vs.* $(T/T_g)^{-1}$. This consideration resulted in a novel concept of fragility of liquids [31]. The larger the fragility parameter *m*, the bigger the change in viscosity with temperature and the bigger the ΔC_p. The quantity *m* can be used as the most fundamental parameter in the empirical classification of viscous liquids. It will be very important to clarify the physical meaning of *m* from a molecular point of view.

Interplay between phase and glass transitions

Crystals and glasses are the two extremes in our concepts of structural regularity in solids. The nature of transitions that occur in crystals and non-crystalline solids differs very much. Transitions in crystals are of thermodynamic origin and in non-crystalline solids are of kinetic or relaxational nature in origin. Even under such circumstances, there is a close interplay between phase and glass transitions.

There are some mesophases whose structures and properties are intermediate between anisotropic crystals and isotropic liquids. The situation is drawn schematically in Fig. 9. One category of mesophases is an orientationally disordered crystal (ODC) in which the constituent molecules form highly symmetric crystal lattices (fcc, bcc, or hcp). Each molecule has orientational disorder among several equi-energetical directions at each lattice points, and the reorientational motion results in enhancement of the molecular symmetry in time- and space-average. Generally the ODC phase transforms on cooling into an ordered phase which satisfies the third law of thermodynamics. If the transformation is avoided by rapid cooling, however, the reorientational motion is immobilized below some temperature 'T_g' in the undercooled ODC phase. This was found for the first time to happen in a cyclohexanol crystal in the undercooled fcc phase [32]. The results are drawn in Fig. 10.

The situation is similar in the preparation of glasses by rapid cooling of liquids. The only difference is the translational invariance with respect to the centres-of-masses the molecules in the orientationally frozen-in state. Thus a 'glassy crystal' has frozen-in degrees of orientational freedom, while keeping the periodical arrangements with respect to the molecular centres-of-masses. The relaxational behaviour observed around 'T_g' is essentially the same as those in liquids. In this way, the freezing process takes place whenever the relaxation time for a particular motion crosses the experimental time-scale. Obviously such glassy crystals will retain a definite amount of residual entropy associated with the frozen-in orientational disorder [33].

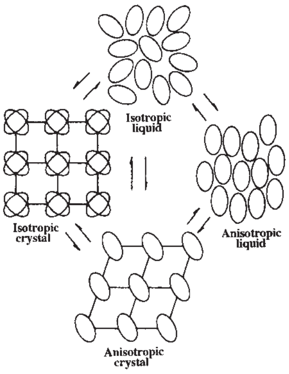

Fig. 9 Schematic drawing of mesophases. Isotropic crystal (plastic crystal) and anisotropic liquid (liquid crystal)

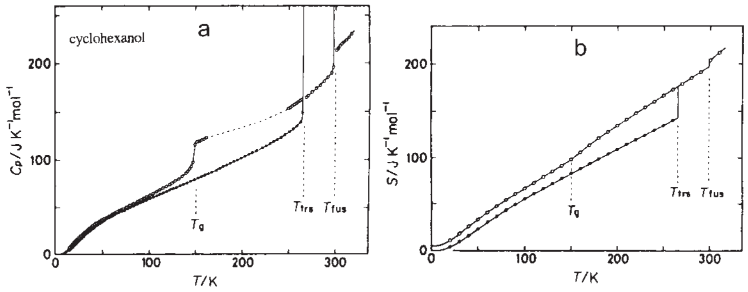

Fig. 10 Heat capacity (a) and entropy (b) of cyclohexanol

Some liquid crystals, counterparts of the mesophases, also exhibit the glass transition and associated residual entropy in the undercooled phase realized by avoiding the transformation into a crystalline phase.

It can be concluded that the glass transition is not a characteristic property of liquids but of wide occurrence in condensed matters in relation to freezing out of some molecular motions owing to prolonged relaxation times for motion at low temperatures [34]. It comes to pass that some aspects of the system cannot maintain an equilibrium state during continuous cooling. This situation is not limited to the cases of metastable undercooled phases. Deviations of ice I_h and CO crystals from the third law of thermodynamics are the most familiar examples of freezing-out of reorientational motions in the stable crystalline phases. The freezing-out of the motion necessary for the realization of an ordered phase surely takes place before the crystal reaches the hypothetical ordering temperature. Such freezing processes can be detected also by dielectric measurements in which orientation polarization of a polar molecule is found to cease to contribute to the dielectric permittivity below certain temperatures that depend on the frequency of the external electric field. The dielectric relaxation time extrapolated to T_g is approximately 1 ks, which is approximately equal to the time-scale necessary for a single heat capacity determination.

Ice I_h forms an ideal three-dimensional hydrogen-bonded system. Each oxygen atom with sp^3 hybridized orbitals uses two of these orbitals to combine with protons and two to provide lone-paired electrons. Four neighbouring oxygen atoms form four hydrogen bonds to the central atom by acting as proton donors, as well as proton acceptors. There are six possible orientations for each water molecule in this structure. The ice crystal has the remarkable property that reorientation of an H_2O molecule is strongly correlated with that of its neighbours. For a configurational change to take place in the disordered lattice, a ring of a least six water molecules has to reorient in unison. The strong correlation arises from the ‘ice rules’, as has been stated earlier. It is this highly cooperative nature which causes a slowing down of the motion at low temperatures, as is evidenced by the dielectric relaxations that have been studied extensively by many scientists.

A small amount of particular impurity doped into the ice lattice was found to accelerate dramatically the motion of water molecules. This will be due to formation of a kind of orientation defect which infringes the ice rules and relaxes the severe constraints imposed on the cooperative motion. Thus, an ice sample doped with KOH in the mole fraction of 10^{-5} exhibited a first-order phase transition at 72 K in an otherwise frozen-in disordered phase [35]. The transition removed a substantial fraction of the residual entropy and changed the space group of the lattice from $P6_3/mmc$ (hexagonal) to $Cmc2_1$ (orthorhombic). The low-temperature ordered phase has anti-polar arrangements of the water dipoles along the c-axis of the original hexagonal ice and is designated as ice XI, following the discoveries of ice modifications over a range of temperatures and pressures.

The same dopant was also effective in inducing ordering transitions in several clathrate hydrates which are composed of hydrogen-bonded water cages enclathrating a guest molecule of an appropriate size [36]. The most familiar cages are dodecahedral 5^{12}, tetradecahedral $5^{12}6^2$ and hexadecahedral $5^{12}6^4$ cavities. For example, the unit cell of type II clathrate hydrates is composed of 16 dodecahedral and 8 hexadecahedral cages, formed by 136 water molecules connected to each other through the hydrogen bonds. Most of the guest species in the type II hydrates are encaged only in the larger cages of $5^{12}6^4$, so that the stoichiometric formula for the full occupation of a guest molecule M is $M\cdot(136/8)H_2O$ or $M\cdot17H_2O$. In this case, the transition temperature was found to depend on the nature of the dipolar guest molecule. Some examples of the anomalous heat capacity associated with the ordering transition are shown in Fig. 11.

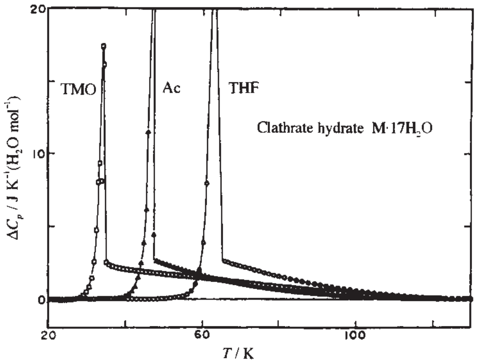

Fig. 11 Anomalous heat capacities associated with phase transitions in tetrahydrofurane (THF), acetone (Ac), and trimethylene oxide (TMO) clathrate hydrates

The dipolar energies among the host water molecules and those among the guest species are considered to couple with each other to determine the structure of the ordered phase. These observations suggest a new realm of science to be called ‘doping chemistry’. Particular kinds of dopants acts on frozen-in disordered systems as catalysts for releasing the immobilized frozen-in state and recovering the equilibrium state. This will surely lead to shortening of the observation times which cannot be long enough in some cases owing to our limited life-span. Glassy crystals are promising and intriguing states of aggregation of molecules that undoubtedly bridge the world of crystals as simple ordered systems and that of liquids as complex disordered systems. Examples of glassy crystals in which the freezing occurs in the metastable or the stable states, examined by our group, are listed in Table 1 along with their glass transition temperatures [37].

Concluding remarks

All materials can be obtained, in principles as the crystalline as well as the non-crystalline states. Only a part of the range of non-crystalline solids, mainly composed of oxides and chalcogenides, has been used in modern technology. There might be many classes of non-crystalline solids that have potential utility in our life. Molecular alloys with divergent compositions, hence with various properties, can possibly be formed by solid-state amorphization processes, as in the case of metallic alloys. In fact, a molecular alloy between deoxycholic acid and tri-O-methyl-β-cyclodextrin crystals (which are hard to believe to form a solid solution [38]) was found recently to form by a mechanical milling process at room temperature. The vitreous mixture exhibited a single glass transition phenomenon with a maximum T_g at the equimolar composition. Formation of solid solutions in molecular crystals under equilibrium conditions is highly limited by many factors, such as the same crystal structures, similar unit-cell sizes, similar molecular shapes and so on [39]. The formation of molecular alloys is possible only under non-equilibrium conditions, and the solution undergoes phase separation on devitrification that occurs above their singe T_g. The combinations of molecular crystals are innumerable and the formation of molecular alloys will find many technical applications. These observations will surely widen the class of non-crystalline solids and enrich our materials science.

Table 1 List of glassy crystals and their glass transition temperatures

Metastable phase		T_g/K	Stable phase	T_g/K
thiophene		37	thiophene	42
2,3-dimethylbutane		76	Buckminsterfullerene C_{60}	87
isocyanocyclohexanol		55	β-cyclodextrin·$11H_2O$	150
		130	ethylene oxide·$6.86H_2O$	85
		160	tetrahydrofuran·$17H_2O$	85
$CFCl_2$–$CFCl_2$		60	acetone·$17H_2O$	90
		90	CO	18
		130	RbCN	30
ethanol		90	$CsNO_2$	42
cyclohexane	I	92	$TlNO_2$	60
	II	93	$SnCl_2$·$2H_2O$	150
cycloheptane	I	100	$SnCl_2$·$2D_2O$	155
	II	100	H_2O (hexagonal)	105
	III	93	H_2O (cubic)	140
cycloheptatriene		106	D_2O (hexagonal)	115
cycloheptanol		135	pinacol·$6H_2O$	155
cyclohexanol		150	H_3BO_3	290
$Cs_{0.7}Tl_{0.3}NO_2$		48	D_3BO_3	298
			lysozyme	ca 150
			myoglobin	ca 170

One of the delayed developments in the science of non-crystalline solids is the lack of structural information, as has been stated earlier. There is another important reason. Many students, even in graduate courses, are not familiar with this subject. This lack of familiarity is simply because the topic has been ignored almost entirely in undergraduate courses. It is hard to find any textbooks on physics or physical chemistry which devote some pages to the subject.

Just after World War II, we were embarrassed by serious shortages of natural textiles. This crisis was saved by rapid development of polymer science. Many of the synthetic polymers are mixtures of crystalline and non-crystalline parts and provide examples of systems which do not obey the phase rule. This is because the rule requires the existence of a single phase over a range of temperatures and pressures in any pure substance. Polymeric materials are in non-equilibrium states from the thermodynamic point of view. Interestingly, we can control the ratio of both parts by thermal annealing which modifies the properties of a polymer without changing its composition. Now we must proceed to the field of fully non-crystalline solids for seeking new functions. It will be necessary to start with one or two lectures on fundamental and phenomenological aspects of the glassy-state to students in high school and in undergraduate courses of university when their brains are quite flexible. Teachers in physical chemistry should not expect the lectures to be given by specialists in this field's, or should the topic be left to other different courses. Strike while the iron is hot.

* * *

Most of the experimental work presented here was done at Osaka University, when the author was in active service. The author would like to express his sincere thanks to many colleagues and students for their enthusiastic collaborations and fruitful discussions.

References

1 N. G. Parsonage and L. A. K. Staveley, Disorder in Crystals, Clarendon Press, Oxford 1978.
2 K. Suenaga, T. Matsuo and H. Suga, Thermochim. Acta, 163 (1990) 263.
3 J. Timmermans, J. Phys. Chem. Solids, 18 (1961) 1.
4 K. Suenaga, T. Matsuo and H. Suga, J. Chem. Thermodyn., to be published.
5 M. Oguni, T. Matsuo, H. Suga and S. Seki, Bull. Chem. Soc. Jpn., 48 (1975) 379; 52 (1979) 941.
6 A. Y. Krasnikova, V. A. Koptsik, B. A. Strukov and W. Ming, Sov. Phys. Solid State, 9 (1967) 85.
7 N. Onoda-Yamamuro, O. Yamamuro, T. Matsuo and H. Suga, to be published.
8 J. Skalo and S. A. Friedberg, Phys. Rev. Lett., 13 (1964) 133.
9 M. E. Fisher, Rep. Prog. Phys., 30 (1967) 615.
10 T. Matsuo, M. Tatsumi, H. Suga and S. Seki, Bull. Chem. Soc. Jpn., 47 (1974) 57.
11 J. D. Bernal and R. H. Fowler, J. Chem. Phys., 1 (1933) 515.
12 M. Tatsumi, T. Matsuo, H. Suga and S. Seki, Bull. Chem. Soc. Jpn., 52 (1979) 716; 52 (1979) 728.
13 S. R. Salinas and J. F. Nagle, Phys. Rev., B9 (1974) 4920.
14 H. Kiriyama, O. Nakamura and R. Kiriyama, Chem. Letters, (1976) 689.
15 N. Arai, M. Sorai, H. Suga and S. Seki, J. Phys. Chem. Solids, 38 (1977) 1341.
16 S. Brawer, Relaxation in Viscous Liquids and Glasses, Am. Ceram. Soc. Inc., Columbus, Ohio 1988.
17 J. D. Mackenzie ed. Modern Aspects of the Vitreous State, Butterworths, London 1964.
18 I. Tsukushi, O. Yamamuro and H. Suga, J. Thermal Anal., 37 (1991) 1143; J. Non-cryst. Solids, 175 (1994) 187.
19 T. Uchino and Z. Yoko, J. Chem. Phys., 108 (1989) 8130; Phys. Rev., B58 (1998) 5322.
20 H. Suga and T. Matsuo, Pure and Appl. Chem., 61 (1989) 1123.
21 R. Kohlrausch, Ann. Phys. (Leipzig) 12 (1847) 393; G. Williams and D. C. Watts, Trans. Faraday Soc., 66 (1970) 80.
22 K. Takeda, O. Yamamuro and H. Suga, J. Phys. Chem., 99 (1995) 1602.
23 H. Hikawa, M. Oguni and H. Suga, J. Non-cryst. Solids, 101 (1988) 90.

24 O. Mishima, J. Chem. Phys., 100 (1994) 5910; Nature, 384 (1996) 546.
25 H. Tanaka, Nature, 380 (1996) 328.
26 P. H. Poole, F. Sciortino, U. Essmann and H. E. Stanley, Nature, 360 (1992) 324.
27 G. Adam and J. H. Gibbs, J. Chem. Phys., 43 (1965) 139.
28 A. J. Kovacs, Fortschr. Hochpolym.-Forsch., 3 (1963) 394.
29 M. Sugisaki, K. Adachi, H. Suga and S. Seki, Bull. Chem. Soc. Jpn., 41 (1968) 593.
30 A. Q. Tool and C. G. Eichlin, J. Am. Chem. Soc., 54 (1931) 491.
31 C. A. Angell, J. Non-cryst. Solids, 130 (1991) 131.
32 K. Adachi, H. Suga and S. Seki, Bull. Chem. Soc. Jpn., 41 (1968) 1073.
33 W. Kauzmann, Chem. Rev., 43 (1948) 219.
34 H. Suga, J. Chem. Thermodyn., 25 (1993) 463.
35 Y. Tajima, T. Matsuo and H. Suga, Nature, 299 (1982) 810; J. Phys. Chem. Solids, 45 (1984) 1135.
36 H. Suga, T. Matsuo and O. Yamamuro, Supramol. Chem., 1 (1993) 221.
37 H. Suga and S. Seki, J. Non-cryst. Solids, 16 (1974) 171; Disc. Faraday Soc., No. 69 (1980) 221, Royal Chem. Soc.
38 S. Furukawa, M. Nagahama and H. Suga, High Temp.-High Press, in press.
39 A. I. Kitaigorodsky, Mixed Crystals, Springer, Berlin 1984.